Comparison of dynamical behaviours of two motorcycle's models in the simulation of lowside fall

ANDREA BONCI, RICCARDO DE AMICIS, SAURO LONGHI AND EMANUELE LORENZONI
Università Politecnica delle Marche
Dipartimento di Ingegneria dell'Informazione
Via Brecce Bianche 12, 60131 Ancona
ITALY
{a.bonci, r.deamicis, sauro.longhi}@univpm.it, emanuele.lorenzoni@tin.it

Abstract: The study and analysis of motorcycle's critical driving situations, falls and accidents, are difficult to be described analitically because of the simultaneity of different and complex phenomena which make the dynamics quite elaborate. However, the controllers for active safety systems of motorcycles cannot be synthesized regardless by a suitable analytic model of the vehicle dynamic. In this paper, an analytic model able to describe the strong nonlinearities conveyed by the complex dynamic of a two-wheeled vehicle in curve, is presented. The model takes into account the coupling between the in-plane and out-of-plane dynamics which is accounted for the system nonlinear behaviour, the rear traction and the nonlinear features of the tyres dynamics. The major steps taken to derive such a model are described. Two sets of motion equations with different levels of accuracy have been developed making use of two different linearizations. The first one is obtained as linearization with respect to the roll and the steer angle around the vertical position, while the second is given by the linearization with respect to the steer angle only. A comparison between the two models for a given initial condition have been made by simulating a real scenario representing a critical vehicle condition, the lowside fall. Results show how these two models have no substantial differences in the description of the low side major dynamics making the simpler model a feasible choice for a model-based design of motorcycle's control system.

Key–Words: Motorcycle dynamic, active safety systems, model-based control systems

1 Introduction

Nowadays, in the automobile industry, active safety systems have reached a high technological level and reliability. On the contrary, that has not happened for the powered two wheelers (PTW), where the most used available system is the Anti-lock Braking System (ABS) [1]. According to recent statistics on motorcycles and mopeds fatalities [2], these kind of systems are desirable to increase rider safety. Currently, the control system design of safety devices for PTWs represents a challenging task.

Model-based design of control systems, widely used in automotive and aerospace sectors, represents an efficient and suitable approach to cope with this challenge [3]. Briefly, the model-based design approach for control systems requires the following steps: the modeling of the plant, the synthesis of the controller for the plant, its simulation and the controller deployment.

In such approach, the plant modeling is a core issue, mainly for systems having complex dynamic behaviours such as automobiles and motorcycles. In particular, the analysis of the motorcycle dynamics is even more complex. While the study of the automobile stability can be addressed adequately by considering the lateral and yaw degrees of freedom, for a motorcycle it is also required to add the roll and the steer angles.

When a motorcycle is leaned over in cornering, the longitudinal and lateral friction forces acting on the tyre-road contact point interact each other and this interaction increases with increased roll angle [4]. As a consequence of this feature, simple mathematical models are not suitable to describe high cornering accelerations during critical situations such as accidents and falls.

In literature [5], analytical models addressing the issues related to motorcycle's behaviour in curve usually makes some major assumptions such as: steady state cornering condition, the longitudinal and lateral contact forces acting on the tyres are linearized or do not interact each other [6]. In general, these works investigate on the effects related to the balancing of forces and moments during a turn as shown in Figure 1, where for a roll angle ϕ the relevant forces (frictional X, Y, centrifugal and gravitational mg) acting

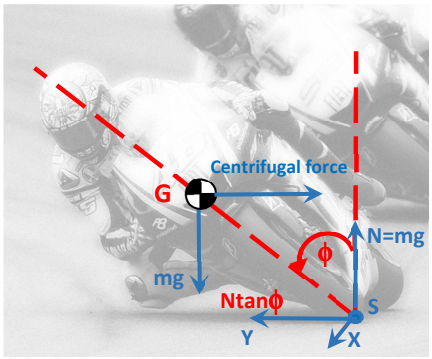

Figure 1: Motorcycle in cornering condition.

on the vehicle system are reported. Their balancing yields the value of the lateral force Y needed to maintain in equilibrium the vehicle in curve that is equal to $N \tan \phi$, where N is the vertical load. However, falls and critical conditions cannot be captured under the aforementioned assumptions when strong acceleration or braking occur. As a result, a controller able to prevent falls should be synthesized by using more appropriate models. On the other hand, commercial multibody software allow to simulate adequately these complicated phenomena, but due to their black box nature they are not suitable for the purpose of synthesis of control systems.

In this paper, after a brief introduction of a classical linear analytical model well known in literature, two nonlinear analytical models with different complexity are described and compared. They are supposedly able to capture the main nonlinearities conveyed by the motorcycle dynamic during falls. Namely, the vehicle's motion equations, yielded by lagrangian formulation, are linearized with repect to the roll angle and the steer angle. That operation gives the first nonlinear model. The second one is derived by linearizing the equation of motions with respect to the steer angle only, hence it represents a more accurate and complex alternative for the motorcycle modelling.

A comparison between the models aforementioned has been made in order to investigate how the different linearization affects the model capability of capturing certain nonlinearities due to the dynamics of the motorcycle in critical fall. Furthermore, this analysis allows to better understand whether the simpler model can possibly represent a righteous trade-off between complexity and accuracy, which is a required feature in the model-based synthesis of stability controller for motorcycles.

The paper is organized as follows: the problem addressed is described in section 2. A description of the geometry of the motorcycle's nonlinear model is summarized in section 3. The steps needed to derive its equations of motion and a nonlinear model for the contact forces are given in section 4. The formulations of all the models derived in this paper are given in section 5. A brief description of the lowside phenomenon and the simulations results are presented in section 6. Section 7 concludes the paper.

2 Problem statement and related works

Active safety systems for motorcycles cannot be synthesized regardless by a suitable dynamic model of the vehicle. The model should be able to describe its behaviour even during falls. Now, the following questions arise. Which analytical model may be suitable to describe the dynamics of the vehicle in complex situations such as the fall during cornering? What is the right trade-off between simulation accuracy and model's complexity? This article proposes the analysis of the results obtained by simulating a typical PTW fall described with a motorcycle's analytic model. The model has the minimum degree of complexity needed to describe these dynamics (two rigid bodies) and two different assumptions of accuracy have been made on it: the roll angle dynamic in both conditions linear and nonlinear have been considered. The comparison of the two behaviours shows the effects of the roll angle dynamic on the accuracy of the results of the model during fall situations when roll angles are involved.

An analytical model is used to address the lowside phenomenon whose complex dynamics usually requires the use of multibody software. The model is based on the author's prior works. It removes the condition of steady-state in cornering and introduces the rear traction given by the engine, the tyre friction forces and their interaction. The proposed model has been already tested in several less critical situations: in [8] the motorcycle dynamics in straight running, acceleration and braking with slippages have been considered; furthermore, the cornering situation with no slippages has been analyzed; in [9] the author's model has been compared with a well established model proposed in literature considering the motorcycle in cornering condition with no slippages; in [10] the same model has been compared with its nonlinear version with respect the lean angle, here the pure rolling during the cornering has been assumed for both the wheels. In this paper a further analysis of the model in critical cornering condition with slippages has been done.

Generally the analytical study and analysis of critical driving situations, falls and accidents, is a complex task since these events take place due to the simultaneity of different circumstances involving the

trim of the motorcycle in motion, the speed and the increase of the lean angle. This analytical complexity augments when considering the loss of adherence both in acceleration and braking that may lead the panicked rider to the typical lowside fall. A lowside may occur while approaching a curve with excessive velocity and braking. Due to the wheels loss of adherence, the rider loses the vehicle control and they both fall laterally.

3 Geometry of the model

As shown in Figure 2, the model uses a multibody approach and it has been developed in an analytical way: the considered motorcycle consists of two longitudinally symmetric rigid bodies which, by means of appropriate constraints, interact each other:

- the rear frame, represented by its mass centre G_r, includes the engine, the petrol tank, the seat, the rear wheel with radius R_r and the rider;
- the front frame, represented by its mass centre G_f and constrained to the rear frame by means of a revolute joint. It includes the handlebars, the fork, the steering mechanism and the front wheel with radius R_f.

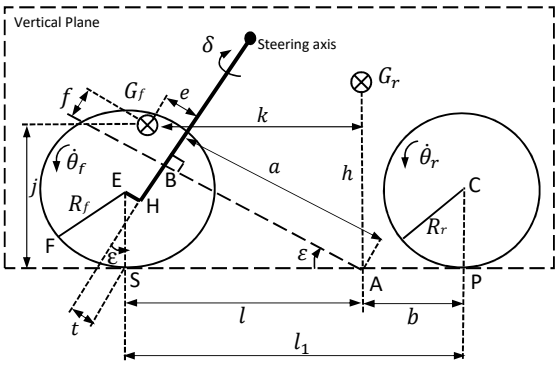

Figure 2: Geometric parameters of the model.

Besides, the main geometric parameters are the heights of the two mass centres h and j respect to the ground level, the wheel base l_1 i.e. the distance between the contact points P and S and the distances of the wheels from the point A, l and b respectively. Lastly, the steering mechanism is described by the steering head angle ϵ and the normal trail t.

Each rigid body has 6 degrees of freedom (dofs) q, of which 5 are inhibited by the joint:

$$q = 6 \times 2 - 5 = 7. \tag{1}$$

In conclusion, the model that considers the motorcycle composed of two rigid elements has at least 7 dofs. The dofs chosen are: the longitudinal and lateral velocity of the motorcycle respectively $\dot{x}_1$, $\dot{y}_1$, the yaw rate $\dot{\psi}$, the roll angle ϕ, the rotation around the steer δ and the angular velocities $\dot{\theta}_r$, $\dot{\theta}_f$. Moreover, the motorcycle moves on a flat road surface, the effects of suspensions are not considered here and the vertical and pitch motions are neglected. The latter assumpions are not restrictive for the comparative analysis proposed in the next sections as the considered models work in the same conditions. Figure 3 shows the

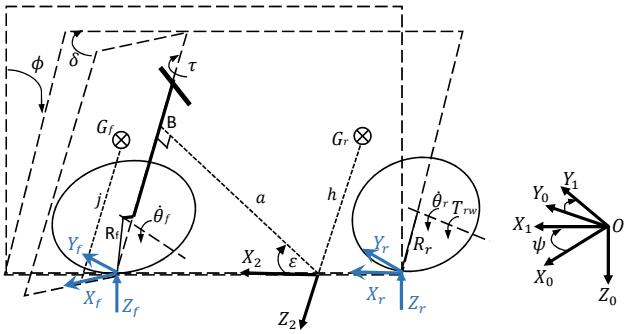

Figure 3: The reference frames.

reference frames needed to describe the position and orientation of the two rigid bodies G_r and G_f as reported in table 1. The transformation matrices allowing to switch between coordinate systems are given by:

reference frame (r.f.)	description
$\Sigma_0(O, X_0, Y_0, Z_0)$	inertial reference frame
$\Sigma_1(O, X_1, Y_1, Z_1)$	rear reference frame rotating Σ_0 of a yaw angle ψ wrt Z_0
$\Sigma_2(O, X_2, Y_2, Z_2)$	rear reference frame rotating Σ_1 of a roll angle ϕ wrt X_1
$\Sigma_3(O, X_3, Y_3, Z_3)$	rear reference frame rotating Σ_2 of a pitch angle ϵ wrt Y_2
$\Sigma_4(O, X_4, Y_4, Z_4)$	front reference frame rotating Σ_3 of a steer angle δ wrt Z_3

Table 1: The reference frames.

$$R_\psi = \begin{bmatrix} \cos\psi & -\sin\psi & 0 \\ \sin\psi & \cos\psi & 0 \\ 0 & 0 & 1 \end{bmatrix}$$
$$R_\phi = \begin{bmatrix} 1 & 0 & 0 \\ 0 & \cos\phi & -\sin\phi \\ 0 & \sin\phi & \cos\phi \end{bmatrix}$$
$$R_\epsilon = \begin{bmatrix} \cos\epsilon & 0 & \sin\epsilon \\ 0 & 1 & 0 \\ -\sin\epsilon & 0 & \cos\epsilon \end{bmatrix} \tag{2}$$
$$R_\delta = \begin{bmatrix} \cos\delta & -\sin\delta & 0 \\ \sin\delta & \cos\delta & 0 \\ 0 & 0 & 1 \end{bmatrix}.$$

In literature, most of the analytical models dealing with a motorcycle in cornering consider the vehicle in steady-state conditions [5], hence situations such as acceleration and braking in curve are not fairly covered. The model herein presented is able to describe these conditions by including the input torque T_{rw} provided by the rear engine. Furthermore, the rider is rigidly attached to the rear body and he maneuvers the motorcycle by applying the torque τ on the handlebar. Finally, referring to Figure 3, X_f, Y_f, X_r and Y_r are the longitudinal and lateral friction forces applied on the tyre-ground contact points S and P respectively, depicted in Figure 2.

4 Equations of motion

After defining the geometry and the model reference frames, the equations of motion can be derived by solving the set of Lagrange's equations described by:

$$\frac{d}{dt}\left(\frac{\partial T}{\partial \dot{q}}\right) - \frac{\partial T}{\partial q} + \frac{\partial V}{\partial q} = Q_q, \tag{3}$$

where:

- $q = [x_1\ y_1\ \psi\ \phi\ \delta\ \theta_r\ \theta_f]^T$ is the system's dofs vector;
- $T(\dot{q}, q)$ is the total kinetic energy of the system;
- $V(q)$ is the total potential energy of the system;
- $Q_q(\dot{q}, q, u)$ is the vector of the generalized external forces acting on each dof $q_i \in q$, $i = 1 \dots 7$;
- $u = [\tau, T_{rw}]^T$ is the inputs vector.

In order to derive the equations of motion, the system (3) must be solved. The given geometry of the system and the hypothesis introduced in prior section make it possible to approach the solution analitically despite all the features taken into account by the model. However, the analytical representation of the solution of (3) gives a set of lengthy equations which cannot be reported here due to space limitations. In the following, the procedure needed to derive these equations will be provided. The procedure aforementioned involves the computing of the total kinetic energy T, the potential energy V and the generalized forces Q_q of the whole system.

4.1 The kinetic energy

In this subsection we derive the expression for the total kinetic energy of the system. It is given by the sum of the kinetic energies of the two rigid bodies composing the system:

$$T = T_r + T_f. \tag{4}$$

where the subscripts $\{r, f\}$ denotes the rear and the front respectively. For each rigid body including the wheels, it is possible to write:

$$\begin{aligned} T_r &= T_r^* + T_{\omega_{rw}} \\ T_f &= T_f^* + T_{\omega_{fw}} \end{aligned} \tag{5}$$

where T_r^* and T_f^* are the kinetic energies of the bodies and $T_{\omega_{rw}}$ and $T_{\omega_{fw}}$ are the wheels rotational kinetic energies not accounted for by T_r^* and T_f^*. Detailing the expressions T_r^* and T_f^* it gives:

$$T_r^* = \frac{1}{2} M_r\, v_r^2 + \frac{1}{2} I_r\, \omega_r^2 \tag{6a}$$

$$T_f^* = \frac{1}{2} M_f\, v_f^2 + \frac{1}{2} I_f\, \omega_f^2, \tag{6b}$$

where M_r, M_f are the masses of the rigid bodies, v_r, v_f are the translational velocities of mass centres G_r and G_f, ω_r, ω_f are the angular velocities of mass centres G_r and G_f, I_r, I_f are the moments of inertia of the rigid bodies while $T_{\omega_{rw}}$ and $T_{\omega_{fw}}$ are the extra terms due to the rotational kinetic energies of the wheels. In the next paragraphs, the energies T_r^*, T_r^*, $T_{\omega_{rw}}$ and $T_{\omega_{fw}}$ will be computed.

4.1.1 The kinetic energy of rear body

Referring to Figure 4, taking into account all the degrees of freedom of G_r, the longitudinal and lateral velocity of the motorcycle $\dot{x}_1$, $\dot{y}_1$, the roll ϕ and yaw

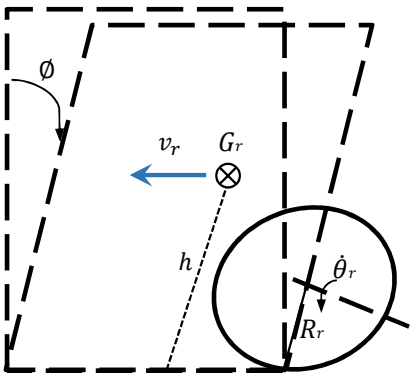

Figure 4: Geometry of rear rigid body.

ψ angles, the translational velocity v_r is:

$$v_r = \begin{bmatrix} \dot{x}_1 - h\sin\phi\dot{\psi} \\ \dot{y}_1 + h\cos\phi\dot{\phi} \\ h\sin\phi\dot{\phi} \end{bmatrix}, \tag{7}$$

in which h represents the height of G_r from the ground considering the vehicle in vertical position. In

a similar way the angular velocity ω_r is:

$$\omega_r \triangleq \begin{bmatrix} p_r \\ q_r \\ r_r \end{bmatrix} = \begin{bmatrix} \dot{\phi} \\ \sin\phi\dot{\psi} \\ \cos\phi\dot{\psi} \end{bmatrix}. \quad (8)$$

Because the axes of reference frame $\Sigma_2(O, X_2, Y_2, Z_2)$ are not parallel to the principal axes through mass centre G_r, the motorcycle's matrix I_r is given by:

$$I_r = \begin{bmatrix} I_{rx} & 0 & -C_{rxz} \\ 0 & I_{ry} & 0 \\ -C_{rxz} & 0 & I_{fz} \end{bmatrix}. \quad (9)$$

Sobstituting the expressions (7), (8) and (9) in (6a), the rear kinetic energy is:

$$T_r^* = \tfrac{1}{2} M_r[(\dot{x}_1 - h\sin\phi\dot{\psi})^2 + (\dot{y}_1 + h\cos\phi\dot{\phi})^2 + (h\sin\phi\dot{\phi})^2] + \tfrac{1}{2} I_{rx} p_r^2 + \tfrac{1}{2} I_{ry} q_r^2 + I_{rz} r_r^2 - C_{rxz} p_r r_r. \quad (10)$$

The wheel is a rigid part of the rear body and it rotates along the y-axis with velocity $\dot{\theta}_r$, so its rotational kinetic energy is:

$$T_{\omega_{rw}} = i_{ry}\left(q_r\dot{\theta}_r + \frac{1}{2}\dot{\theta}_r^2\right), \quad (11)$$

where i_{ry} is its polar moment of inertia. Adding the latter's contribution to (10), the total kinetic energy of the rear frame T_r becomes:

$$T_r = \tfrac{1}{2} M_r[(\dot{x}_1 - h\sin\phi\dot{\psi})^2 + (\dot{y}_1 + h\cos\phi\dot{\phi})^2 + (h\sin\phi\dot{\phi})^2] + \tfrac{1}{2} I_{rx}\dot{\phi}^2 + \tfrac{1}{2} I_{ry}(\sin\phi\dot{\psi})^2 + I_{rz}(\cos\phi\dot{\psi})^2 - C_{rxz}\cos\phi\dot{\phi}\dot{\psi} + i_{ry}\left(\sin\phi\dot{\psi}\dot{\theta}_r + \tfrac{1}{2}\dot{\theta}_r^2\right). \quad (12)$$

4.1.2 The kinetic energy of front body

Similarly, by repeating the same steps formerly described for the rear kinetic energy, after calculating the translational velocity v_f and the angular velocity ω_f of mass centre G_f, the front kinetic energy is given by:

$$T_f = \tfrac{1}{2} M_f[(\dot{x}_1 - e\cos\epsilon\sin\delta\dot{\delta} - (a\sin\epsilon\sin\phi + e\sin\delta\cos\phi + e\sin\epsilon\cos\delta\sin\phi + f\cos\epsilon\sin\phi)\dot{\psi})^2 + (\dot{y}_1 + a\sin\epsilon\cos\phi\dot{\phi} - e\sin\delta\sin\phi\dot{\phi} + e\cos\delta\cos\phi\dot{\delta} + e\sin\epsilon\cos\delta\cos\phi\dot{\phi} - e\sin\epsilon\sin\delta\sin\phi\dot{\delta} + f\cos\epsilon\cos\phi\dot{\phi} + (a\cos\epsilon + e\cos\delta\cos\epsilon - f\sin\epsilon)\dot{\psi})^2 + (a\sin\epsilon\sin\phi\dot{\phi} + e\sin\delta\cos\phi\dot{\phi} + e\cos\delta\sin\phi\dot{\delta} + e\sin\epsilon\cos\delta\sin\phi\dot{\phi} + e\sin\epsilon\sin\delta\cos\phi\dot{\delta} + f\cos\epsilon\sin\phi\dot{\phi})^2] + \tfrac{1}{2} I_{fx}[(\cos\epsilon\cos\delta\dot{\phi} + \sin\delta\sin\phi - \sin\epsilon\cos\delta\cos\phi)\dot{\psi}]^2 + \tfrac{1}{2} I_{fy}[-\cos\epsilon\sin\delta\dot{\phi} + (\cos\delta\sin\phi + \sin\epsilon\sin\delta\cos\phi)\dot{\psi}]^2 + \tfrac{1}{2} I_{fz}[\dot{\delta} + \sin\epsilon\dot{\phi} + \cos\epsilon\cos\phi\dot{\psi}]^2 + i_{fy}[(-\cos\epsilon\sin\delta\dot{\phi} + (\cos\delta\sin\phi + \sin\epsilon\sin\delta\cos\phi)\dot{\psi})\dot{\theta}_f + \tfrac{1}{2}\dot{\theta}_f^2], \quad (13)$$

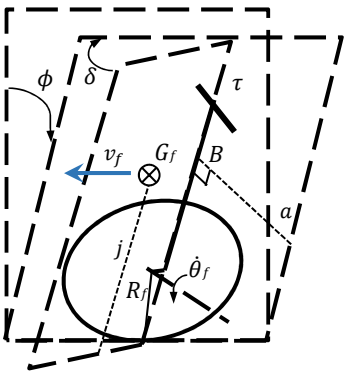

Figure 5: Geometry of front rigid body.

where:

$$i_{fy}[(-\cos\epsilon\sin\delta\dot{\phi} + (\cos\delta\sin\phi + \sin\epsilon\sin\delta\cos\phi)\dot{\psi})\dot{\theta}_f + \tfrac{1}{2}\dot{\theta}_f^2] \quad (14)$$

represents the extra term $T_{\omega_{fw}}$ due to the front wheel rotational kinetic energy. Adding up the expressions (12) and (13) it yields the total kinetic energy of the system.

4.2 Potential energy

The potential energy of the system is the sum of the potential energies of the two rigid bodies. Indicating with V the total potential energy and with V_r and V_f, the rear and front ones respectively, we can write:

$$V = V_r + V_f = M_r g z_r + M_f g z_f, \quad (15)$$

where g is the gravitational acceleration and z_r and z_f are the heights of G_r and G_f respect to the ground. According to the orientations of the vehicle represented in figures 4 and 5 the potential energy is given by:

$$V = M_r g h\cos\phi + M_f g(a\sin\epsilon\cos\phi - e\sin\phi\sin\delta + e\sin\epsilon\cos\delta\cos\phi + f\cos\epsilon\cos\epsilon). \quad (16)$$

In the next subsection the vector of the generalized forces appearing in equation (3) will be computed.

4.3 Generalized forces

The next step to solve the system (3) requires the computing of the vector of the generalized forces Q_q. Its components act on each dof $q_i \in q$ and is given by:

$$Q_q = [Q_{x_1}, Q_{y_1}, Q_\psi, Q_\phi, Q_\delta, Q_{\theta_r}, Q_{\theta_f}]. \quad (17)$$

If q_i has the dimension of a length, the corresponding generalized force Q_{q_i} is a force, while if q_i has the dimension of an angle, the corresponding generalized force Q_{q_i} is a torque.

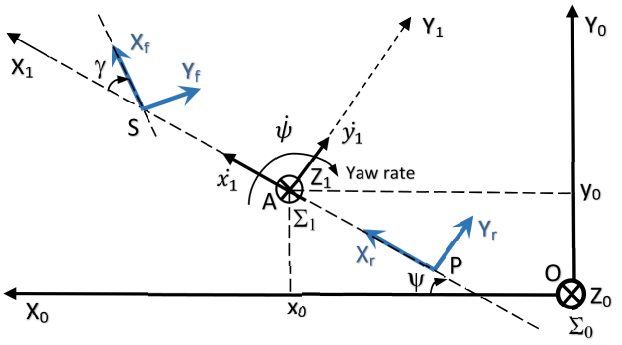

Figure 6: Top view of motorcycle showing the tyre forces in the ground plane.

In order to make easier the computation of Q_{x_1} and Q_{y_1} the reader can refer to Figure 6. By defining $[X_i;\, Y_i;\, Z_i]^T$ the forces acting on the tyre contact point, where the subscript $i = r, f$ indicates the rear or the front tyre, the generalized forces are computed simply by considering the balance of the forces along the x and y-axes:

$$\begin{aligned} Q_{x_1} &= X_r + X_f \cos\gamma - Y_f \sin\gamma \\ Q_{y_1} &= Y_r + Y_f \cos\gamma + X_f \sin\gamma, \end{aligned} \tag{18}$$

where the parameter γ is the effective front wheel steer angle.

Referring to Figure 3 and considering the subset $q^* = [\psi,\ \phi,\ \delta,\ \theta_r,\ \theta_f]$ of q, and $Q_q^* = [Q_\psi, Q_\phi, Q_\delta, Q_{\cdot\theta_r}, Q_{\theta_f}]$ of Q_q, it yields:

$$\begin{aligned} Q_\psi &= l\, Y_f - Y_r\, b \\ Q_\phi &= -t \sin\delta (Z_f \cos\phi - Y_f \sin\phi) \\ Q_\delta &= -K\dot{\delta} + t[\{(X_f \cos\gamma - Y_f \sin\gamma)\cos\epsilon \\ &+ (Y_f \sin\phi - Z_f \cos\phi)\sin\epsilon\}\sin\delta \\ &- (Y_f \cos\phi + Z_f \sin\phi)] + \tau \\ Q_{\theta_r} &= -T_{rw} + R_r X_r \\ Q_{\theta_f} &= R_f X_f, \end{aligned} \tag{19}$$

where Q_q^* are the torques acting on the vehicle, T_{rw} is the rear traction, τ is the torque applied by the rider to the handlebar, K is a generic steering damper coefficient, b, l and t are parameters listed in table 2.

In order to determine the expression of the angle γ refer to Figure 7 that shows the front wheel in some generally displaced position. Introducing a unit vector

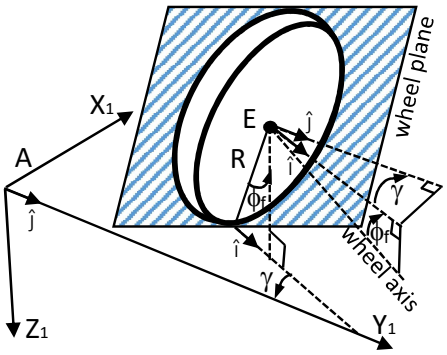

Figure 7: The front camber angle.

$\hat{i}$ directed along the y-axis of the wheel:

$$\hat{i} = \begin{bmatrix} -\sin\delta\cos\epsilon \\ \cos\delta\cos\phi - \sin\delta\sin\epsilon\sin\phi \\ \cos\delta\sin\phi + \cos\phi\sin\delta\sin\epsilon \end{bmatrix} \tag{20}$$

the angle γ can be easily computed from the components of (20):

$$\tan\gamma = -\frac{i_x}{i_y} = \frac{\sin\delta\cos\epsilon}{\cos\delta\cos\phi - \sin\delta\sin\epsilon\sin\phi}. \tag{21}$$

The unknown friction forces X_r, Y_r, X_f, Y_f of (18) and (19) will be computed in the next paragraph, while as anticipated in the assumptions, the vertical motion is neglected and then the forces $Z_r = Z_f = Z$ have constant value as reported in table 2.

4.4 The contact forces

In order to describe the motorcycle behaviours on a curve and in critical situations, the tyre friction forces have to be modeled adequately. Indeed, they transfer the power provided by the engine through the tyre-ground contact and they are needed to push the vehicle and keep it in balance while running the trajectory in curve.

Literature proposes several tyre models [14], among which, purely theoretical models such as the brush model can be found [11]. This model is able to describe most of the tyre conditions. Other kinds of models are empirical hence they do not provide any theoretic foundamentals but deliver accurate descriptions of the tyres behaviour. Among the empirical models, the "magic formula" became the standard for the vehicle dynamic simulations [12]. The model is described by the following expression:

$$\begin{aligned} y(x) = ZD \sin(C \arctan\{Bx \\ - E[Bx - \arctan(Bx)]\}), \end{aligned} \tag{22}$$

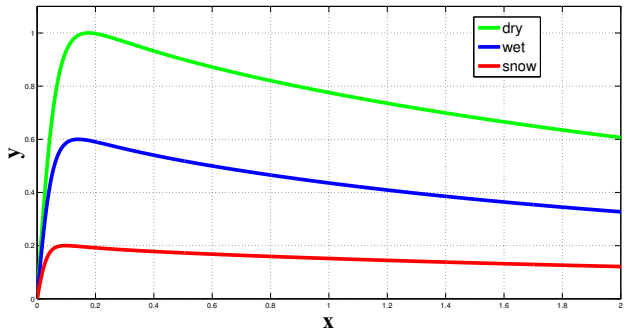

Figure 8: The magic formula for different road conditions.

where the variables and parameters in the equation are: x is the input variable, y is the output variable and B, C, D and E represent the curve parameters describing the road adhesion conditions as shown in Figure (8). The equation (22) allows to calculate:

- the longitudinal forces X_r and X_f as a function of the longitudinal slip;
- the lateral forces Y_r and Y_f as a function of the lateral slip and roll angles.

Based on the SAE J670 definitions, the longitudinal slip λ_i is defined as:

$$\lambda_i = -\frac{\dot{x}_i - R_i\dot{\theta}_i}{\dot{x}_i}, \tag{23}$$

where $\dot{x}_i$, $\dot{\theta}_i$ and R_i are respectively the wheel forward velocity, the wheel angular velocity and the wheel's radius and the subscript $i = f, r$ refers to front and rear tyre. The coefficient λ_i is positive in traction and negative in the case of braking. The lateral slip α_i is defined as:

$$\alpha_i = -\arctan\frac{\dot{y}_i}{\dot{x}_i}, \tag{24}$$

where $\dot{x}_i$ and $\dot{y}_i$ are the forward and lateral velocity of the wheel. Using expressions (23) and (24), the magic formula (22) for the longitudinal force holds:

$$X_{0i} = Z\,D_x \sin(C_x \arctan\{B_x\lambda_i - E[B_x\lambda_i - \arctan(B_x\lambda_i)]\}), \tag{25}$$

where λ_i is given by (23). For motorcycle tyres, the roll angle (or camber angle) can reach up to $50°$-$55°$ in extremis cases. In order to take into account the lateral slip and the camber angle, it is possible to define the so-called equivalent sideslip as:

$$\alpha_{ieq} = \alpha_i + \frac{k_\phi}{k_\alpha}\phi_i, \tag{26}$$

where α_i is the lateral slip defined in (24), ϕ_i is the wheel camber angle, k_ϕ and k_α are respectively the camber and the cornering stiffnesses. Using the equivalent sideslip (26), the lateral force becomes:

$$Y_{0i} = Z\,D_y \sin(C_y \arctan\{B_y\alpha_{ieq} - E[B_y\alpha_{ieq} - \arctan(B_y\alpha_{ieq})]\}). \tag{27}$$

Besides, for a tyre running a curve, when both the longitudinal and lateral forces are present, it is possible to describe their interaction by considering the following theoretical slips quantities:

$$\begin{cases} \sigma_{xi} = \dfrac{\lambda_i}{1+\lambda_i} \\ \sigma_{yi} = \dfrac{\tan\alpha_{ieq}}{1+\lambda_i}, \end{cases} \tag{28}$$

whose module is:

$$\sigma_i = \sqrt{\sigma_{xi}^2 + \sigma_{yi}^2}. \tag{29}$$

Therefore, making use of the expressions (28) and (29), the friction forces hold:

$$\begin{cases} X_i' = \dfrac{\sigma_{xi}}{\sigma_i} X_{0i} \\ Y_i' = \dfrac{\sigma_{yi}}{\sigma_i} Y_{0i}, \end{cases} \tag{30}$$

where X_{0i} and Y_{0i} are given by (25) and (27). Finally, to take into account the elasticity of the tyres the following equations must be introduced:

$$\begin{cases} \dfrac{\xi_x}{\dot{x}_1}\dot{X}_i + X_i = X_i' \\ \dfrac{\xi_y}{\dot{x}_1}\dot{Y}_i + Y_i = Y_i', \end{cases} \tag{31}$$

where ξ_x and ξ_y are the tyre longitudinal and lateral relaxation lengths and X_i' and Y_i' are given by (30). The expressions of X_i and Y_i computed in (31) for the rear and front tyre are the friction forces of the model showed in Figure 3.

5 Formulation of the motorcycle models

In the previous sections all the variables needed to compute the equations of motion and the forces for the motorcycle's model have been explained. Briefly, sobstituting in (3) the kinetic energy T, the potential energy V and the generalized forces Q_q given in (4), (15), (18) and (19), a set of 7 nonlinear second order differential equations are obtained. Furthermore the expressions (31) describing the dynamics of the contact forces X_r, X_f, Y_r and Y_f, add 4 more

nonlinear first order differential equations to the system. Using the dofs q, it is possible to define the state vector X_q as:

$$X_q = [\phi\ \delta\ \dot{x}_1\ \dot{y}_1\ \dot{\psi}\ \dot{\phi}\ \dot{\delta}\ \dot{\theta}_r\ \dot{\theta}_f]^T. \tag{32}$$

Besides, by defining the contact forces vector X_F as:

$$X_F = [X_r\ X_f\ Y_r\ Y_f]^T, \tag{33}$$

it is possible to represent the whole nonlinear system in a general state-space representation:

$$S: \begin{cases} \dot{X}_q = f_1(X_q, u) & \text{(34a)} \\ \dot{X}_F = f_2(X_F) & \text{(34b)} \end{cases}$$

where $u = [\tau\ T_{rw}]^T$ are the external input. The subsystem (34a) represents the set of 7 nonlinear lagrangian equations of the system (3) and the subsystem (34b) represents the 4 nonlinear equations of the contact forces expressed in (31).

As introduced in section 2, such a system delivers lenghty and complex equations, hard to be managed. Its usage as a model in designing a controller is to be excluded. However, this model could be considered as a validation tool for less accurate models that should be used for that purpose. Therefore, in this paper, the system S will be represented as the starting point for further derivations and analysis of models with different accuracy.

In order to find a reliable analytical model for the purpose of this paper, three kind of models could be derived from the system S. A first one has been widely investigated in literature [7], but it is of poor practical interest to the purposes of this paper. This model has the lowest accuracy and the simpler analytical equations. It has been obtained assuming the vehicle at constant longitudinal speed and only small perturbations from straight running are considered. Since the longitudinal velocity of the vehicle is assumed to be constant, the longitudinal dynamics disappear and the longitudinal tyre forces X_r and X_f become zeros. In addition, the tyres vertical load Z has been considered constant and no slippages occur. Under these assumptions the subsystems (34a) and (34b) have been linearized with respect to the roll and the steer angle around the vertical position $(\phi, \delta) = (0, 0)$. Defining the state vector $x = [\phi \delta \dot{y}_1 \dot{\psi} \dot{\phi} \dot{\delta} Y_r Y_f]^T$, the nonlinear model (34) leads to the following time invariant linear system:

$$S_1 : \dot{x} = A_1(\dot{x}_1)\, x + B_1 \tau, \tag{35}$$

in which $\dot{x}_1$ is the longitudinal speed of the vehicle. Matrix $A_1(\dot{x}_1)$ and B_1 are reported in appendix. Matrix $A_1(\dot{x}_1)$ only depends on the constant longitudinal speed $(\dot{x}_1)$ hence the simulations in acceleration or braking situations are not possible. Moreover, analytical models such as (35) are too simple and then not able to capture the strong nonlinearities that arise in cornering conditions where the coupling between the in-plane and out-of plane dynamics has to be considered. Based on the aformentioned observations, this model is excluded from further analysis.

A second kind of model S_2 has been derived from (34) by linearizing the equations of motion (34a) with respect to the roll and steer angles around the vertical position $(\phi, \delta) = (0, 0)$. A nonlinear model for the friction forces and their interactions have been considered (equations (31)). Finally by introducing the rear engine traction T_{rw} has allowed the description of the motorcycle dynamics in acceleration and braking in straight running or in cornering and the coupling between the longitudinal and lateral dynamics. Defining the state vector $x = [\phi\ \delta\ \dot{x}_1\ \dot{y}_1\ \dot{\psi}\ \dot{\phi}\ \dot{\delta}\ \dot{\theta}_r\ \dot{\theta}_f\ X_r\ X_f\ Y_r\ Y_f]^T$, leads to the nonlinear system in the state and affine in the input, having dynamics:

$$S_2 : \dot{x} = A_2(x)\, x + B_2\, u, \tag{36}$$

where the matrices $A_2(x)$ and B_2 are reported in Appendix. As shown, despite the small angle assumption, matrix $A_2(x)$ is continuous $(C^k, k \geq 0)$ and $B \neq 0\ \forall x$. In particular there are two kind of nonlinearities: the products $\dot{x}_i \dot{x}_j$ which represent the centrifugal effects when $i = j$ and the Coriolis effects when $i \neq j$. These kind of effects are inherent nonlinear phenomena and arise directly from the kinetic energy T of the system 4. Furthermore, the additional nonlinearities are due to the trigonometric functions $\sin(\cdot)$ and $\arctan(\cdot)$ describing the friction forces X_i' and Y_i' and their interaction.

The third model S_3, derived from the system (34), is the more accurate. It is used in this paper for testing the model S_2 by comparison in the simulation of a critical motorcycle dynamic. This model is given by linearizing the system S with respect to the angle δ. The roll dynamics is kept non linear as well as the friction forces dynamics. For a motorcycle on a curve the steer angle δ remains limited to a few degrees endorsing the linearization assumption, while the lean angle ϕ usually can assume large values, then the small approximation for the roll angle may be excessive. Therefore, linearizing the steer angle δ and defining the same state vector x as for the system (36), it yields:

$$S_3 : \dot{x} = A_3(x, cos\phi, sin\phi)\, x + B_3\, u. \tag{37}$$

Due to the lenght of the matrix $A_3(x, \cos\phi, \sin\phi)$, system S_3 is not reported in this paper. In addition to the properties previously described for $A_2(x)$,

in $A_3(x, \cos\phi, \sin\phi)$ the roll dynamic is entirely described by the functions $\cos\phi$ e $\sin\phi$.

Their behavior will be compared and the results will be shown in the next paragraph.

6 Lowside fall simulations

A motorcycle may experience a lowside fall while entering in a curve with excessive speed and instinctively the rider brakes hard to keep the trajectory. The

Figure 9: The lowside fall. (Source: www.zimbio.com)

strong rear braking results in the rear wheel losing lateral adherence and the increase of the roll and yaw angles. In case the panicking rider ignores the loss of adherence and keeps on braking, the slippage never stops because the lateral force acting on the rear wheel is always lesser than the force necessary to keep the vehicle in balance. In particular, the required friction force is proportional to $\tan\phi$ (Figure 1). In this case the roll angle increases progressively and the vehicle ends up to fall laterally and drag the rider down (Figure 9).

In the following it will be investigated the effect of the roll angle on the motorcycle dynamic by simulating the vehicle during a lowside fall and comparing the behaviour of the linearized model against the nonlinear model. In the following figures the trends of the variables involved in the simulations are compared. The subscripts "L" and "NL" stand for the linear and the nonlinear case respectively, "r" and "f" stand for rear and front. The trajectory, the roll angle ϕ, the yaw angle ψ, the lateral forces Y_r and the longitudinal forces X_r acting on the rear wheel, the rear wheel's angular velocity $\dot{\theta}_r$, the front wheel's angular velocity $\dot{\theta}_f$ have been compared. The simulations start with the motorcycle runnnig the trajectory depicted in Figure 10. The vehicle engages the curve at 40 m/s (144 km/h) with roll angle ϕ of about 40°, as shown in Figure 12.

The trends of the variables yield by the linear model and the nonlinear model are very similar till

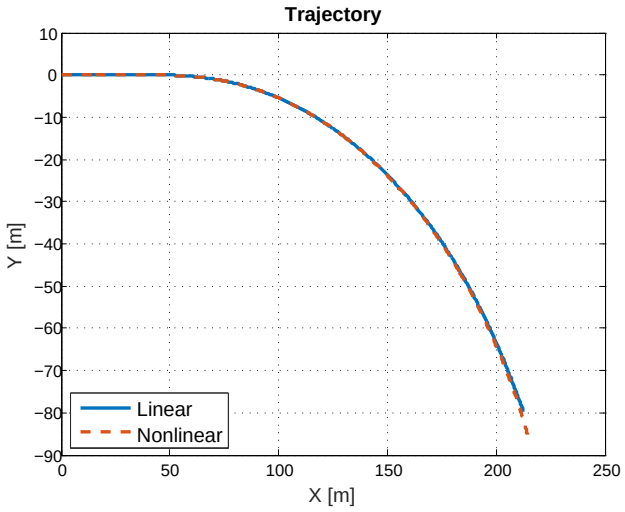

Figure 10: The curve.

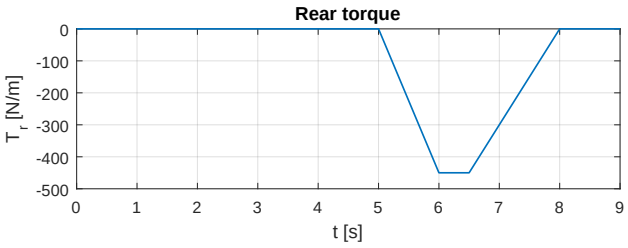

Figure 11: The rear torque.

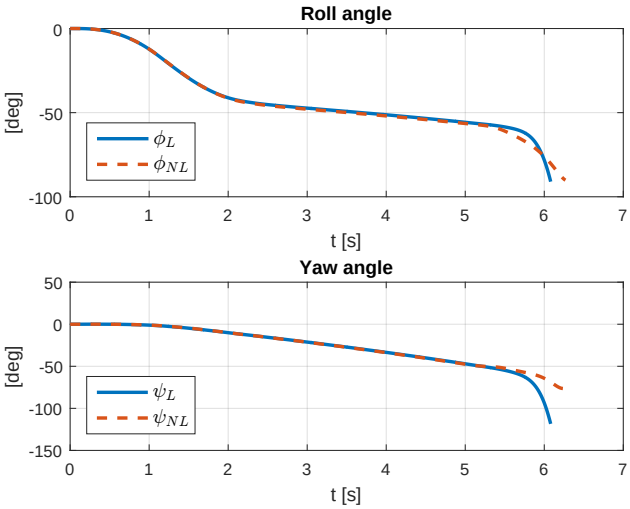

Figure 12: The roll and yaw angles.

the brake is applied. Figure 11 shows the strong negative rear torque applied on the rear wheel in the time window 5-6.5 seconds. This torque simulates the hard braking applied by the rider. As shown in Figure 13,

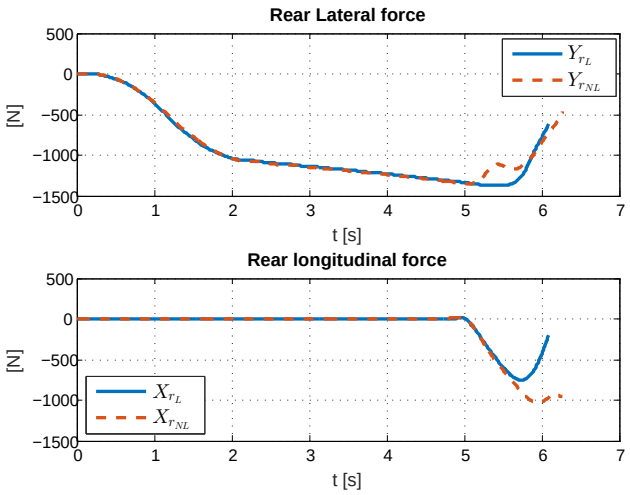

Figure 13: The rear lateral and longitudinal forces.

during the same time window the longitudinal forces X_{r_L}, $X_{r_{NL}}$ acting on the rear wheel (also known as the braking forces) show a fast growing trend as expected. Figure 14 shows that the braking action leads

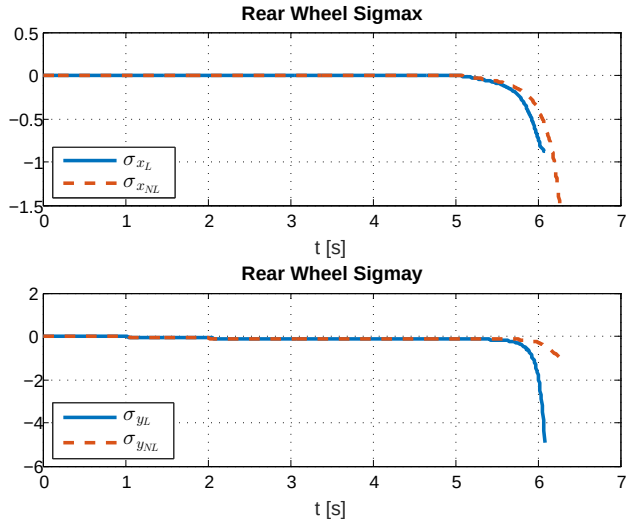

Figure 14: The rear theoretical slips.

to an increase in the rear longitudinal slip angles σ_{x_L}, $\sigma_{x_{NL}}$. As a result of the longitudinal slip, the rear lateral slips σ_{y_L}, $\sigma_{y_{NL}}$ increase as well because the rear lateral force Y_r needed to maintain the vehicle in balance are reached with a greater rear slip angle in both linear and nonlinear cases. The rear wheel's angular velocities $\dot{\theta}_{r_L}$, $\dot{\theta}_{r_{NL}}$ decrease more strongly with respect to the relevant front wheel's angular velocities $\dot{\theta}_{f_L}$, $\dot{\theta}_{f_{NL}}$ (Figure 15). As the braking force reaches

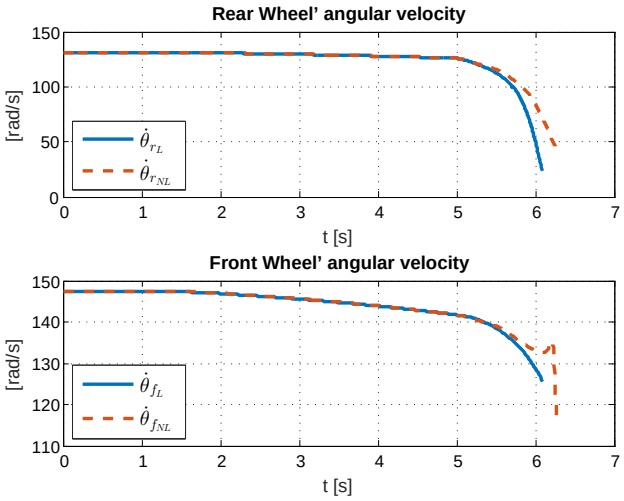

Figure 15: The rear and front angular velocities.

its maximum at 6 seconds (Figure 11), a slight difference on the rear wheel's angular velocities can be observed between the linear and nonlinear cases, but still they maintain the same trend. The roll angles drop progressively in both cases although the trends are slightly different as shown in Figure 12. In Figure 13 the lateral forces Y_{r_L} and $Y_{r_{NL}}$ acting on the rear wheel are shown. During the braking, the force Y_{r_L} starts decreasing more rapidly than $Y_{r_{NL}}$ but in both cases these values tend to decrease progressively and they are not sufficient to keep the motorcycle in balance hence the slip angle of the rear wheel continues to grow as well as the roll angles ϕ_L and ϕ_{NL}. At 6.5 seconds the rider starts decelerating but the roll angle has now reached such a value that it is impossible for the rider to regain the correct attitude of the vehicle in both cases. Indeed, around 6.2 seconds the motorcycle reaches 90° in the roll angle hence it falls down and the simulation ends. The trajectories depicted in

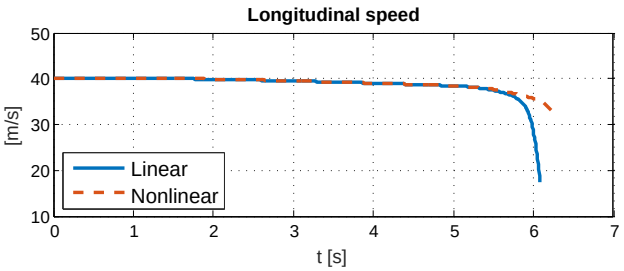

Figure 16: The longitudinal velocity.

Figure 10 show little difference between the linear and the nonlinear case, precisely in the first case the fall occurs slightly sooner than in the nonlinear case. The graphs clearly show that the linearization on the roll

angle ϕ is able to describe most of a lowside fall dynamic, in particular this event occurs slightly in advance respect to the nonlinear case, but the trajectory run by the vehicles are very similar. The major difference stands on the final longitudinal velocity that in the linear case reaches a smaller value (Figure 16). It is worth noting that the general vehicle dynamic in this critical condition is strongly affected by the tyres friction forces. The trends of the dynamics variables obtained in the simulations are in line with what was expected. This results push the authors to address a deeper analysis of the model in future works.

7 Conclusion

The most of the works dealing with motorcycle's dynamic simulation and synthesis of controllers are being carried out with the aid of software multibody and at the best of author's knowledge, simulations of critical situations such as the lowside fall have never been treated by means of analytical tools. In order to plug this lack, in this paper a nonlinear model of a motorcycle has been presented along with the foundamental steps which are to be taken to derive the set of its differential equations of motions (model S). Given the complexity of such a model, in this paper the analysis has involved other two nonlinear models, herein called S_2,S_3, derived from S and presenting increasing accuracy. The model S_2 represents a nonlinear model derived by linearizing the system S with respect to the roll and steer angles around the vertical position and the modeling of the friction forces has been kept non linear. Such a model is able to capture the most of the motorcycle dynamic with a degree of accuracy which has to be evaluated in the perspective of a possible usage in the design of stability controllers. To this purpose, in this paper, the system $S2$ has been compared with the more accurate model $S3$ in the simulation of the low side fall of a motorcycle. The system $S3$ has been derived by keeping the roll dynamic nonlinear. The comparison of the low side simulation have shown that the model $S2$ is able to capture with fair accuracy the critical phenomenon at issue hence it could represent a good trade-off between complexity and accuracy. Further analysis towards the properties of the system $S2$ have to be investigated in order to evaluate a possible usage of this system in a model-based design of a stability controller.

References:

[1] P. Seiniger, K. Schröter, J. Gail, Perspectives for motorcycle stability control systems, *Accident Analysis & Prevention*, Volume 44, Issue 1, 2012, pp. 74-81.

[2] European Road Safety Observatory, `https://ec.europa.eu/transport/road_safety/specialist/erso_en`

[3] J. Reedy, S. Lunzman, Model Based Design Accelerates the Development of Mechanical Locomotive Controls, *SAE Technical Paper*, 2010.

[4] C. Koenen, The dynamic behaviour of a motorcycle when running straight ahead and when cornering, *PhD Dissertation*, 1983, TU Delft.

[5] V. Cossalter, A. Doria, R. Lot, Steady Turning Of Two Wheel Vehicles, *Vehicle System Dynamics*, 31, 3, 1999, pp. 157-181.

[6] R. Lot, A Motorcycle Tires Model for Dynamic Simulations: Theoretical and Experimental Aspects, *Meccanica*, vol. 39, 2004, pp. 207-220.

[7] R. S. Sharp, The lateral dynamics of motorcycles and bicycles, *Vehicle System Dynamics*, 14, 1985, pp. 265-283, (1985)

[8] A. Bonci, R. De Amicis, S. Longhi, G. A. Scala and A. Andreucci, Motorcycle lateral and longitudinal dynamic modeling in presence of tyre slip and rear traction, *21st International Conference on Methods and Models in Automation and Robotics (MMAR)*, Miedzyzdroje, 2016, pp. 391-396.

[9] A. Bonci, R. De Amicis, S. Longhi, E. Lorenzoni and G. A. Scala, A motorcycle enhanced model for active safety devices in intelligent transport systems, *12th IEEE/ASME International Conference on Mechatronic and Embedded Systems and Applications (MESA)*, Auckland, 2016, pp. 1-6.

[10] A. Bonci, R. De Amicis, S. Longhi, E. Lorenzoni and G. A. Scala, Motorcycle's lateral stability issues: Comparison of methods for dynamic modelling of roll angle, *20th International Conference on System Theory, Control and Computing (ICSTCC)*, Sinaia, 2016, pp. 607–612.

[11] H. Dugoff, P. Fancher, L. Segel, Tire performance characteristics affecting vehicle response to steering and braking control inputs. *Ed. by Michigan Highway Safety Research Institute*, 1969.

[12] A. T. van Zanten, Bosch ESP Systems: 5 Years of Experience, *SAE Technical Paper*, 2000.

[13] R. A. Serway and Jr. J. W. Jewett, Physics for Scientists and Engineers. *9th Ed*, 2013.

[14] J. C. Dixon. Tyres, Suspension and Handling, *Cambridge University Press*, 1991.

A Physical parameters

The motorcycle physical parameters are listed in table 2.

parameter	notation	value	u.m. (SI)
M_f	mass of front frame	30.6472	kg
M_r	mass of rear frame	217.4492	kg
Z	vertical force	-1005.3	N
I_{rx}	rear frame inertia x axis	31.184	$\mathrm{kg\,m^2}$
I_{rz}	rear frame inertia z axis	21.069	$\mathrm{kg\,m^2}$
C_{rxz}	product of inertia xz	1.7354	$\mathrm{kg\,m^2}$
I_{fx}	front frame inertia x axis	1.2338	$\mathrm{kg\,m^2}$
I_{fz}	front frame inertia z axis	0.442	$\mathrm{kg\,m^2}$
$i_{fy} = i_{ry}$	front and rear wheel inertias	0.7186	$\mathrm{kg\,m^2}$
C_{rxz}	product of inertia xz	1.7354	$\mathrm{kg\,m^2}$
ϵ	caster angle	0.4715	rad
a	distance between A and B	0.9485	m
b	distance between A and P	0.4798	m
e	x position of G_r	0.024384	m
f	z position of G_f	0.028347	m
h	z position of G_r	0.6157	m
l	distance between A and S	0.9346	m
R_r	rear wheel radius	0.3048	m
R_f	front wheel radius	0.3048	m
t	trail	0.11582	m

Table 2: Motorcycle physical parameters.

B Dynamical matrices of the derived systems

$$A_1(\dot{x}_1) = \begin{bmatrix} 0 & 0 & 0 & 0 & 1 & 0 \\ 0 & 0 & 0 & 0 & 0 & 1 \\ 9.005 & 0.6321 & 0 & 0.3104\dot{x}_1 & 0.00222\dot{x}_1 & 0.02 - 0.01163\dot{x}_1 \\ -12.1 & -3.382 & 0 & -0.3692\dot{x}_1 & 0.003937\dot{x}_1 & 0.03373\dot{x}_1 + 0.3491 \\ 0.7212 & -0.05211 & 0 & -1.6\dot{x}_1 & -0.02379\dot{x}_1 & 0.01685 - 0.005704\dot{x}_1 \\ 280.6 & 128.8 & 0 & -1.715\dot{x}_1 & 4.58\dot{x}_1 & -0.04993\dot{x}_1 - 15.57 \\ 5441\dot{x}_1 & 0 & -64933 & 31155 & 0 & 0 \\ 3911\dot{x}_1 & 43266\dot{x}_1 & -46566 & -43522 & 0 & 5393 \end{bmatrix}$$

$$\begin{bmatrix} 0 & 0 \\ 0 & 0 \\ -0.006248 & -0.003382 \\ -0.009621 & 0.02997 \\ 0.008337 & 0.003054 \\ 0.02176 & -0.317 \\ -4.101\dot{x}_1 & 0 \\ 0 & -4.167\dot{x}_1 \end{bmatrix} \quad B_1 = \begin{bmatrix} 0 \\ 0 \\ 0.008737 \\ -0.05537 \\ -0.01646 \\ 2.302 \\ 0 \\ 0 \end{bmatrix}$$

$$A_2(x) = \begin{bmatrix} 0 & 0 & 0 & 0 & 0 \\ 0 & 0 & 0 & 0 & 0 \\ 0 & 0 & 0 & \dot{\psi} & 6e^{-3}\dot{\delta} + 0.11\dot{\psi} \\ -27.0 & -1.9 & 0 & 5.8e^{-3}\dot{\psi}\delta & 5.6e^{-3}\dot{\delta}\delta - 0.02\dot{\theta}_r - 1.0\dot{x}_1 - 0.011\dot{\theta}_f + 6.1e^{-4}\dot{\psi}\delta \\ -0.29 & -2.6 & 0 & -0.037\dot{\psi}\delta & 4.7e^{-3}\dot{\theta}_r - 0.015\dot{\theta}_f + 5.6e^{-16}\dot{x}_1 - 1.5e^{-3}\dot{\delta}\delta - 3.9e^{-3}\dot{\psi}\delta \\ 43 & 2.9 & 0 & -0.011\dot{\psi}\delta & 0.017\dot{\theta}_f + 0.033\dot{\theta}_r - 2.0e^{-15}\dot{x}_1 - 9.2e^{-3}\dot{\delta}\delta - 1.2e^{-3}\dot{\psi}\delta \\ 266.0 & 133.0 & 0 & 1.5\dot{\psi}\delta & 0.74\dot{\theta}_f - 0.017\dot{\theta}_r - 6.7e^{-16}\dot{x}_1 + 0.014\dot{\delta}\delta + 0.16\dot{\psi}\delta \\ 0 & 0 & 0 & 0 & 0 \\ 0 & 0 & 0 & 0 & -0.45\dot{\delta} \\ 0 & 0 & 10X'_r & 0 & 0 \\ 0 & 0 & 10X'_f & 0 & 0 \\ 0 & 0 & 4.1Y'_r & 0 & 0 \\ 0 & 0 & 4.2Y'_f & 0 & 0 \end{bmatrix}$$

$$\begin{bmatrix} 1 & 0 & 0 & 0 & 0 & 0 \\ 0 & 1 & 0 & 0 & 0 & 0 \\ 1.2\dot{\psi} & 2.7e^{-3}\dot{\delta} & 0 & 0 & 4.0e^{-3} & 4.0e^{-3} \\ 5.6e^{-3}\dot{\theta}_r - 1.8e^{-3}\dot{\theta}_f - 0.011\dot{\delta}\delta + 0.019\dot{\psi}\delta & 1.6e^{-5}\dot{\delta}\delta - 0.01\dot{\theta}_f - 0.059 & 0 & 0 & 2.3e^{-5}\delta & -4.3e^{-3}\delta \\ 0.017\dot{\theta}_f - 0.027\dot{\theta}_r + 2.6e^{-3}\dot{\delta}\delta - 0.047\dot{\psi}\delta & 0.38 - 9.9e^{-5}\dot{\delta}\delta - 5.6e^{-3}\dot{\theta}_f & 0 & 0 & -1.5e^{-4}\delta & -4.6e^{-3}\delta \\ 7.3e^{-3}\dot{\theta}_f - 4.7e^{-3}\dot{\theta}_r + 0.018\dot{\delta}\delta - 0.033\dot{\psi}\delta & 0.019\dot{\theta}_f - 2.9e^{-5}\dot{\delta}\delta + 0.11 & 0 & 0 & -4.4e^{-5}\delta & 6.7e^{-3}\delta \\ 0.058\dot{\theta}_r - 1.4\dot{\theta}_f - 9.4e^{-3}\dot{\delta}\delta + 1.8\dot{\psi}\delta & 7.5e^{-3}\dot{\theta}_f + 4.1e^{-3}\dot{\delta}\delta - 16.0 & 0 & 0 & 6.2e^{-3}\delta & 0.24\delta \\ -\dot{\psi} & 0 & 0 & 0 & 0.29 & 0 \\ 0.89\dot{\delta} - \dot{\psi} & 0 & 0 & 0 & 0 & 0.42 \\ 0 & 0 & 0 & 0 & -10.0\dot{x}_1 & 0 \\ 0 & 0 & 0 & 0 & 0 & -10\dot{x}_1 \\ 0 & 0 & 0 & 0 & 0 & 0 \\ 0 & 0 & 0 & 0 & 0 & 0 \end{bmatrix}$$

$$\begin{bmatrix} 0 & 0 \\ 0 & 0 \\ 0 & 0 \\ 0.019 & 0.01 \\ -0.018 & 0.026 \\ -0.021 & -0.013 \\ 0.035 & -0.31 \\ 0 & 0 \\ 0 & 0 \\ 0 & 0 \\ 0 & 0 \\ -4.1\dot{x}_1 & 0 \\ 0 & -4.2\dot{x}_1 \end{bmatrix} \quad B_2 = \begin{bmatrix} 0 & 0 \\ 0 & 0 \\ 0 & 0 \\ 8.7e^{-3} & 0 \\ -0.055 & 0 \\ -0.016 & 0 \\ 2.3 & 0 \\ 0 & -0.95 \\ 0 & 0 \\ 0 & 0 \\ 0 & 0 \\ 0 & 0 \\ 0 & 0 \end{bmatrix}$$